



Twin hopping in nanolayered Zr-2.5Nb

Jie-Wen Zhang, Brandon Leu, M. Arul Kumar, Irene J. Beyerlein & Wei-Zhong Han

To cite this article: Jie-Wen Zhang, Brandon Leu, M. Arul Kumar, Irene J. Beyerlein & Wei-Zhong Han (2020) Twin hopping in nanolayered Zr-2.5Nb, Materials Research Letters, 8:8, 307-313, DOI: [10.1080/21663831.2020.1755902](https://doi.org/10.1080/21663831.2020.1755902)

To link to this article: <https://doi.org/10.1080/21663831.2020.1755902>



© 2020 The Author(s). Published by Informa UK Limited, trading as Taylor & Francis Group



[View supplementary material](#)



Published online: 28 Apr 2020.



[Submit your article to this journal](#)



Article views: 455



[View related articles](#)



[View Crossmark data](#)

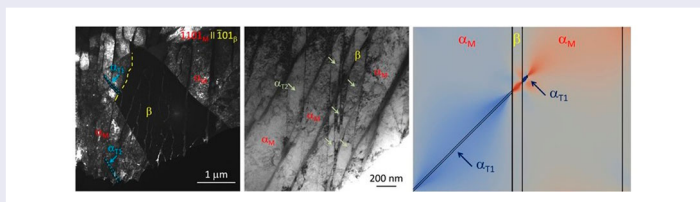
Twin hopping in nanolayered Zr-2.5Nb

Jie-Wen Zhang^a, Brandon Leu^b, M. Arul Kumar^c, Irene J. Beyerlein^{b,d} and Wei-Zhong Han^a

^aCenter for Advancing Materials Performance from the Nanoscale, State Key Laboratory for Mechanical Behavior of Materials, Xi'an Jiaotong University, Xi'an, People's Republic of China; ^bMaterials Department, University of California, Santa Barbara, CA, USA; ^cMaterials Science and Technology Division, Los Alamos National Laboratory, Los Alamos, NM, USA; ^dDepartment of Mechanical Engineering, University of California, Santa Barbara, CA, USA

ABSTRACT

Twinning in coarse-grained Zr is ubiquitous but not in nanostructured Zr due to the strong nanoconfinement. Here we show that hexagonal close-packed (hcp) twins can proliferate in a nanolayered Zr-Nb as a result of the introduction of ductile body centered cubic (bcc) nanolayers. Both common $\{1\bar{1}02\}$ twins and less common $\{1\bar{1}21\}$ twins are found to propagate across the nanolayers by a novel twin hopping mechanism from one hcp layer to another. The fine ductile bcc nanolayers act as buffers that lower the back stress at the hcp/bcc interface far below that which usually constrains twinning.



IMPACT STATEMENT

We report a twin hopping mechanism by which hcp twins are facilitated by the introduction of ductile bcc nanolayers that lessen the back stress and enable the twin to bypass.

ARTICLE HISTORY

Received 11 March 2020

KEYWORDS

Twinning; Zr-2.5Nb;
nanolayer; interface;
plasticity

1. Introduction

Zr-based nanocomposites containing a high density of biphasic interfaces are drawing much attention due to a combination of exceptional strength, corrosion resistance, and radiation tolerance [1–5]. Understanding the unusual interface-enabled mechanisms when these materials are deformed are of critical importance to their widespread implementation as structural components. To date, nanostructured α -Zr have not seen the formation of deformation twins, an otherwise common deformation mechanism in coarse-grained α -Zr [6–10]. Numerous studies on α -Zr and other hexagonal close-packed (hcp) crystals have shown that twinning is promoted during mechanical straining in coarse-grained sample ($> 1 \mu\text{m}$), or under cryogenic temperatures (e.g. liquid nitrogen temperature, 77 K), or at high strain

rates [8–12]. Yet still, even under these special conditions, only a few twin types, namely $\{1\bar{1}02\} < \bar{1}101 >$ and $\{1\bar{1}22\} < \bar{1}123 >$, are predominant, and other types, such as $\{1\bar{1}21\} < 11\bar{2}6 >$ twins, are infrequent [8,13,14].

Twins preferentially originate statistically from grain boundaries and interfaces because these surfaces are ideal sites where both high stresses and crystalline defects can coincide within the same nanoscale volume [7,15–17]. In recent years, increasing attention has been focused on revealing the debilitating effect of bi-phase interfaces, grain boundaries, nano-confinement, and precipitates on twin propagation [18–22]. Due to the strong back stresses imposed by these features back onto the twin boundary, expansion of the twin is curtailed and higher applied stresses are needed to overcome the back stress to continue twin growth.

CONTACT Wei-Zhong Han wzhanxjtu@mail.xjtu.edu.cn Center for Advancing Materials Performance from the Nanoscale, State Key Laboratory for Mechanical Behavior of Materials, Xi'an Jiaotong University, Xi'an 710049, People's Republic of China

Supplemental data for this article can be accessed here. <https://doi.org/10.1080/21663831.2020.1755902>

Here we discover that the α -Zr nanolayers in a two-phase Zr-2.5Nb α/β nanolayered composites deform by both $\{1\bar{1}02\}$ and $\{\bar{1}\bar{1}21\}$ twinning under cryogenic rolling. It is found that these twins proliferate across many alternating α -Zr layers, without any deformation in or transmission through the body centered-cubic (bcc) β nanolayers, indicating that these twins propagate from one α -Zr layer to the next one by *hopping* over the β nanolayers. Using a combination of TEM and 3D crystal plasticity calculations, we elucidate that the periodically spaced β nanolayers stimulate twinning in three key ways. First, they reduce the back stress imposed by the impinging α -twin, and second, their sufficiently fine nanoscale thickness does not deleteriously reduce the twin-tip forward stress, permitting it to continue growing in the next α -Zr layer. Third, once the twin hops to the next α -Zr layer, the original back stress in the first layer converts to a forward stress, catalyzing twin growth.

2. Experimental methods

Hierarchical 3D nanolayered Zr-2.5Nb alloy was synthesized using a thermal mechanical phase transformation method [5]. The Zr-2.5Nb α/β nanolayers have a classic Burgers orientation relationship (OR) of $[0001]_{\alpha} \parallel [011]_{\beta} (\bar{1}\bar{1}20)_{\alpha} \parallel (1\bar{1}1)_{\beta}$ [5]. Two sheets with a size of 10 mm \times 8 mm \times 4 mm were used for cryogenic rolling. The samples were immersed in liquid nitrogen for at least 15 min before each rolling pass. The total rolling reductions for these two sheets are approximately 15% and 25%. Microstructural characterization was carried out using a FEG JEOL 2100F transmission electron microscope (TEM, 200 kV). TEM foils were first ground to a thickness of 50 μm , then further thinned by twin-jet polishing in a solution of 10 vol.% perchloric acid and 90 vol.% ethanol.

3. Results and discussion

Figure 1(a) shows a TEM image of an α/β laminated grain after 25% rolling. The α/β layers have average layer thicknesses of $h_{\alpha} \approx 220$ nm and $h_{\beta} \approx 20$ nm, respectively. The length and width of β layers are several microns and continuously separate α layers. Deformation twins are found to span across multiple α/β lamellae. The twin in the middle is relatively wide and the other twin in the lower left corner in Figure 1(c,d) is a tiny narrow one. Four sections of the twin boundaries in the α layers can be identified according to their contrast difference (marked in Figure 1(a)). The selected area diffraction patterns (SADP) at the twin boundary region (labeled as b in Figure 1(a)) are shown in Figure 1(b). The red dash lines mark the SADP of the α -Zr matrix (α_M), and the

blue dash lines label the SADP of the α twin (α_{T1}). The dark field images corresponding to diffraction spots of $(0001)_M$ and $(0001)_{T1}$ shown in Figure 1(c,d) are used to distinguish α_M and α_{T1} . From these analyses these structures are identified as a $\{1\bar{1}02\}$ twin, a common twin in hcp crystals [7,16,23]. The unusual observation here, however, is that these $\{1\bar{1}02\}$ twins are found in several adjacent α -layers within the same colony, indicating that the nanoscale β layers in between them, did not impede twinning.

To determine how the β layers, between the twinned α layers, deformed, we took an SADP of a set of α/β layers after twinning in α layers with the $[1\bar{1}1]$ zone axis (Figure 1(e)). By comparing with Figure 1(b), we find that the OR between the α_M and β layers in the twinned region remained as original [5]. The new α_{T1}/β interface is nearly parallel to basal plane (0001) of α_{T1} , which corresponds to the 85.2° rotation along $[\bar{1}\bar{1}20]_{\alpha}$ caused by the $\{1\bar{1}02\}$ twin. Figure 1(f) shows the dark field image of the β layers, obtained by selecting $(\bar{1}01)_{\beta}$, and a portion of the twin front that has been impeded by the thin β layer, as marked by the yellow dash line. The β layer has not reoriented, and thus, the α twin has not prompted another twin in the β layer. No steps are found along the α/β interface after twinning. Plasticity is also not obvious inside the β layer during $\{1\bar{1}02\}$ twin formation. Therefore, the new α_{T1}/β interface OR is established via reorienting the α layer to the twin $\{1\bar{1}02\}$ orientation while maintaining the β layer's original orientation.

Figure 2 shows a TEM image of another type of tensile twin after 15% rolling. These twins are thinner, with widths of 30–150 nm, than the $\{1\bar{1}02\}$ twins in Figure 1. Figure 2(b) shows the SADP taken from region marked with b in Figure 2(a) with a zone axis of $[\bar{1}2\bar{1}3]$. These belong to the $\{\bar{1}\bar{1}21\} <11\bar{2}6>$ family of tensile twins. The $[\bar{1}2\bar{1}3]$ zone axis is the invariant zone axis for the $\{\bar{1}\bar{1}21\}$ twin plane and it is seen to lie in the α/β interface. Therefore, the $\{\bar{1}\bar{1}21\}$ twin boundaries and α/β interface are both in edge-on position under this viewing direction. The same $\{\bar{1}\bar{1}21\}$ twin variant exists across multiple α layers. As before, the intervening β nanolayers did not impede twinning in adjacent α layers.

To understand the response of the β layer, we analyze the twinned- α/β interface region. Figure 2(c–f) shows in greater detail the morphologies of the $\{\bar{1}\bar{1}21\}$ twin (α_{T2}) and α/β interface at the intersection point. The $\{\bar{1}\bar{1}21\}$ twin boundaries are severely bent where they contact the β layer (Figure 2(d)). The $\{\bar{1}\bar{1}21\}$ twin becomes thinner as it draws closer to the β layer, a reflection of the strong back stress due to the interaction between the twin and interface (Figure 2(c–d)). In Figure 2(d,f), the yellow dash lines mark the position of the β layer in the $\{\bar{1}\bar{1}21\}$ twinned region. Again, we see that the β nanolayer has

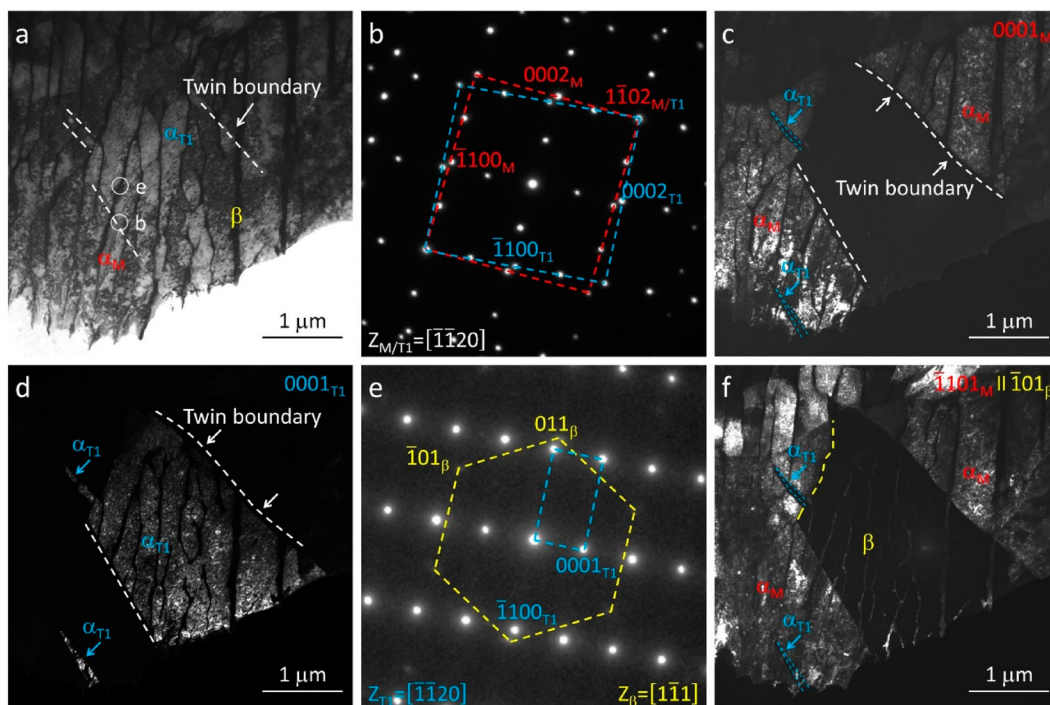


Figure 1. (a) TEM image of a $\{1\bar{1}02\}$ twin crossing the α/β interfaces in the LNT rolled sample to 25% rolling reduction. (b) SADP of the $\{1\bar{1}02\}$ twin obtained from the circle marked in (a). (c–d) DF images using diffraction spots of $(0001)_M$ and $(0001)_{T1}$ in (b). (e) SADP obtained from the circle in (a). (f) DF image using the diffraction spot of $(101)_\beta$ in (e).

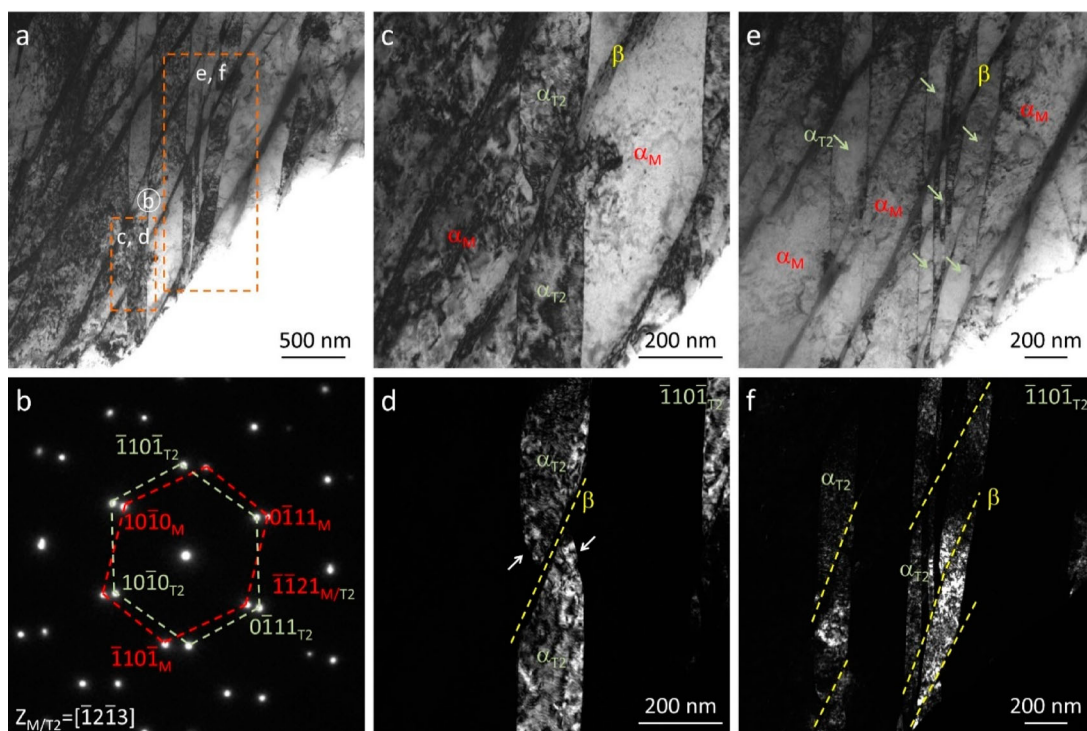


Figure 2. (a) TEM image of a $\{1\bar{1}\bar{1}\}$ twin crossing the α/β interfaces in the LNT rolled sample to 15% rolling reduction. (b) SADP of the $\{1\bar{1}\bar{1}\}$ twin obtained from the circle in (a). (c–f) Magnified images of the regions in (a). DF images in (d) and (f) using the diffraction spot of $(\bar{1}\bar{1}0\bar{1})_{T2}$ in (b).

neither reoriented, slipped, nor twinned in response to the impingement by the $\{\bar{1}\bar{1}21\}$ twin. Figure 2(e–f) shows another region containing several narrow $\{\bar{1}\bar{1}21\}$ twins. The thicker twin in one α -layer is followed by three smaller twins in the next α -layer. The alignment of these twins in separate layers suggests that the thicker twin in one layer prompted multiple twins in the adjacent α layers. However, if this is the case, then twin propagation from one α layer to the next was not enabled by the transmission of dislocations or twins across the α/β interface [15,17], since the intervening β nanolayer did not incur any obvious deformation or reorientation.

Both $\{1\bar{1}02\}$ and $\{\bar{1}\bar{1}21\}$ tensile twins have been reported in coarse-grained pure α -Zr under cryogenic deformation [8–10,24]. Up to now, in traditional unalloyed Zr, $\{1\bar{1}02\}$ and $\{\bar{1}\bar{1}21\}$ tensile twins are typically much finer than the grain size and develop preferentially in larger grains [8]. Twinning usually becomes hindered in grains of sub-micron and nanoscale dimensions [21,22,25]. In addition, twin growth in hcp metals have been observed to become difficult in materials with a high density of precipitates [20]. Twins must bypass or engulf precipitates in order to continue propagating [20]. However, because the width and length of β layers are several microns, the α -twin would not be able to propagate across the same laminated colony by spreading laterally to circumvent the β -layer. Furthermore, the volume fractions of the $\{\bar{1}\bar{1}21\}$ twin type are commonly much lower than that of the $\{1\bar{1}02\}$ twin [8]. Notably, the uncommon $\{\bar{1}\bar{1}21\}$ tensile twins are also observed.

To understand their propagation and interaction with the β nanolayers in the lamellar Zr-2.5Nb, we employed a 3D crystal plasticity approach to calculate the local stress fields produced by the $\{1\bar{1}02\} \langle \bar{1}101 \rangle$ twin. The twin is explicitly formed by the reorientation of the twin domain and the incremental development of the characteristic twinning transformation shear. Details on the simulation are described in Supplementary Materials (see Supplementary Material). The model includes a discrete $\{1\bar{1}02\}$ twin lamella in the α -layer (Figure S1). Twin lamellae naturally grow by migrating their boundary, a process that involves glide of twinning dislocations or climb of disconnections, which are driven by a positive twinning resolve shear stress (TRSS) [26–28]. Twin boundary migration towards twin thickening requires the TRSS to be positive, whereas a negative TRSS would indicate detwinning [26,27]. Thus, observing the TRSS fields that develop from forming the twin lamella can provide insight into where and how the twin is developing. The TRSS of $\{1\bar{1}02\}$ twin is computed as an example below.

Figure 3(a) shows the TRSS field while the $\{1\bar{1}02\}$ twin lies in the α layer prior to contact with the β layer.

Positive stress concentrations (red) develop ahead of the twin tip in α matrix, while negative (dark blue) TRSS evolves in the vicinity of twin boundary. This result is analogous to the TRSS around an isolated twin [26]. This stress state benefits twin propagation but restrains twin thickening. The fields suggest that at this stage, twin remains the same thickness as it grows toward the β layer. Figure 3(b) presents the slip accumulated from all active slip systems (prismatic $\langle a \rangle$, basal $\langle a \rangle$ and pyramidal $\langle c+a \rangle$ slip) distributed in α layer. The plasticity-induced relaxation occurs predominantly at the twin tip but in the α layer only. The β layer, at this stage, experiences no plastic deformation, in agreement with observation in Figure 1.

Figure 3(c) shows the TRSS field once the twin impinges on the β layer. Plasticity in the β layer becomes highly localized and asymmetric, developing immediately inside the β layer, especially at the upper twin boundary- β layer junction (Figure 3(d)). Yet this plastic deformation does not span the width of the β layer, as shown in Figure 3(d). Thus, a mechanism of slip-transmission twinning is unfavorable [29]. Furthermore, dislocation pile-ups, amounting to more than say two dislocations, in the β layers with thickness < 20 nm are not expected. The twin boundary back stress remains negative, and hence resistive stress against further twin growth are present; however, it has been partly relieved locally at the twin- β layer junction, as indicated by red-to-blue arrow in Figure S2(a,b) (see Supplementary Material). Accordingly, with increased applied strain, the twin may thicken where this twin has impinged upon the α/β interface. Along the other α/β interface between the same β layer and the next α layer, the positive TRSS (red) is particularly high opposite the twin- β contact position. In the region of the twin tip in the neighboring α layer, the average TRSS is 106.5 MPa, which is higher than the critical TRSS for twinning, 102 MPa [26], therefore the stress concentration is sufficiently high to trigger a new twin, as highlighted in Figure 3(c).

Figure 3(e) shows the stress state after a new twin embryo is introduced in the second α -layer at the highest stress concentration site. Remarkably, the new twin has caused the twin boundary back stress of the first twin at the first α/β junction to reduce even further and in a few other areas to convert to a twin boundary forward stress, which could promote its expansion, as shown in Figure 3(e) and S2(a,b) (see Supplementary Material). In the adjacent layer, the twin boundary stress of the new twin is a positive forward stress, supporting the propagation of newly formed α twin further into its parent crystal (Figure 3(e)). The β layer experiences highly localized plastic deformation that spans the entire width of β layer (Figure 3(f)). The misorientations calculations in the β

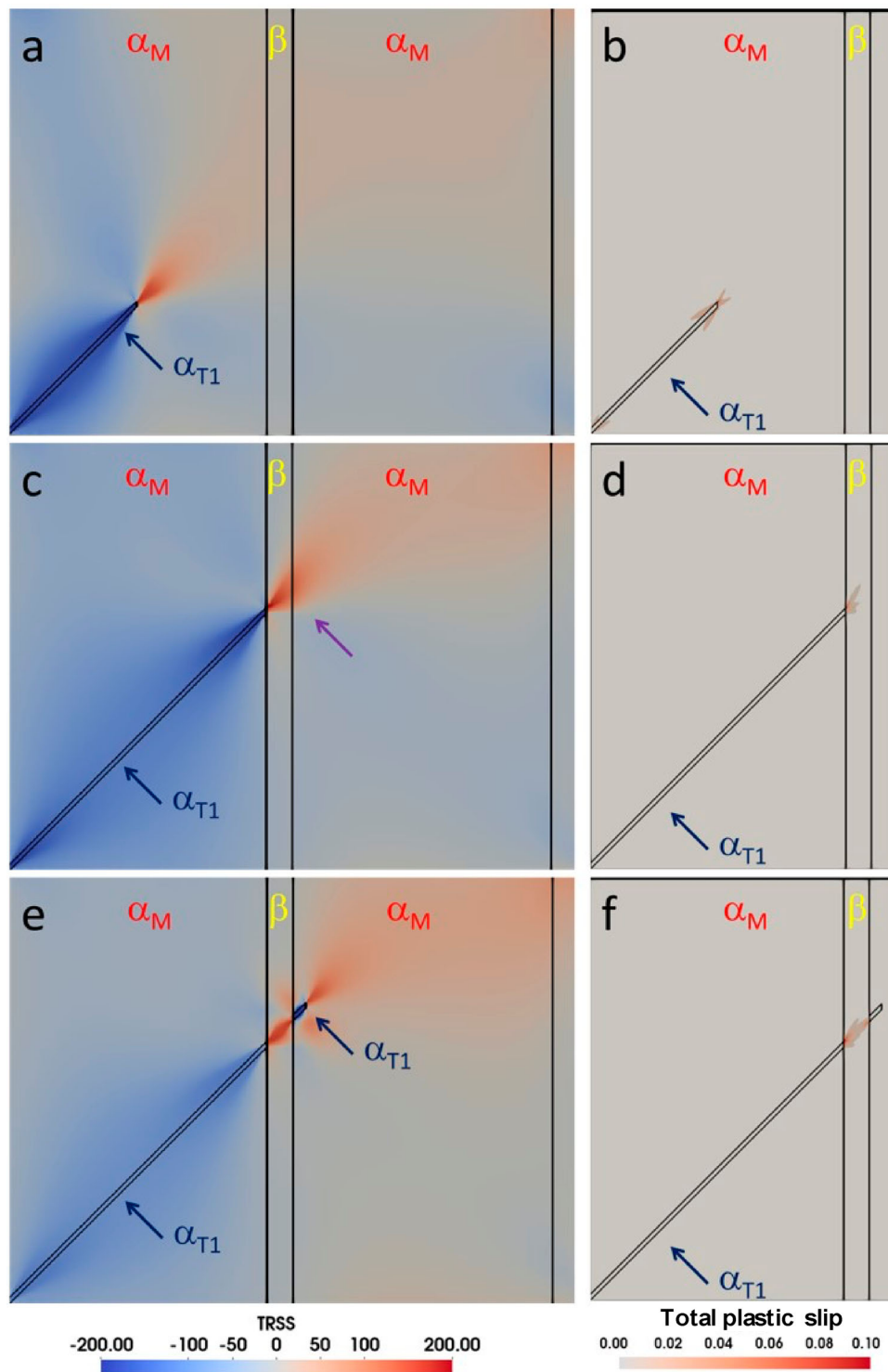


Figure 3. Distribution of the twin resolved shear stress (TRSS) and localized plasticity during twin propagation in the α layer and skipping the β layer. The measure of plasticity is the sum of the accumulated plastic slip among all respective slip systems: basal, prismatic and pyramidal for the α layer and the $\{110\}$ and $\{112\}$ slip for the β layer. (a–b) Prior to $\{1\bar{1}02\}$ twin/ β layer contact. (c–d) At the point of the $\{1\bar{1}02\}$ twin meeting the β layer. (e–f) A new twin produced in the adjacent α layer.

layer indicates no significant reorientation ($< 1^\circ$), consistent with observations in Figure 1. Twinning on both sides of the β layer causes the β layer to yield, resulting in the reduction of the twin boundary back stress that

was originally hindering thickening of the first twin, and promoting continued twinning of the new twin.

In prior calculations on single phase α -Zr, the formation of parallel twins in the same crystal can hinder

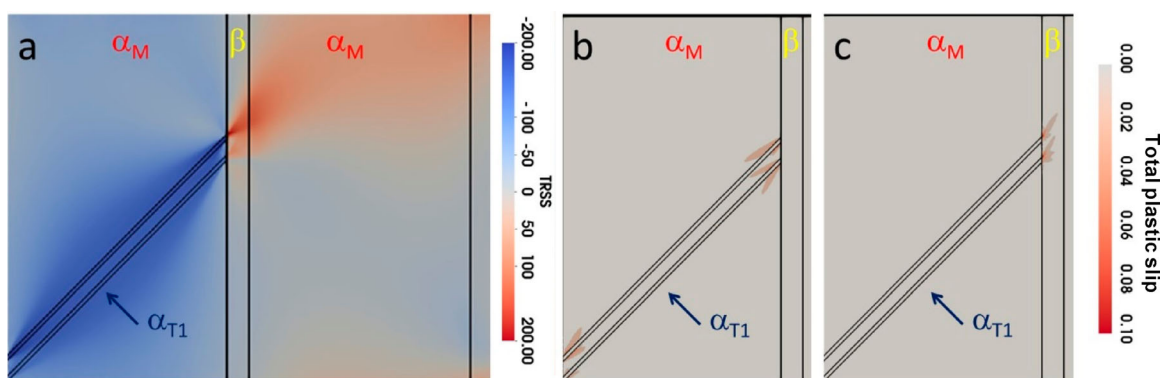


Figure 4. Two parallel $\{1\bar{1}02\}$ twins meeting the β layer. (a) Distribution of the TRSS in the adjacent α layer. (b–c) Localized plasticity or accumulated slip in α and β layer near the $\{1\bar{1}02\}$ twin/ β junction. The total plastic slip is the sum of all slip among the respective slip systems: basal, prismatic and pyramidal for the α layer and the $\{110\}$ and $\{112\}$ slip for the β layer.

each other's thickening and that the smaller their parallel twin spacing, the higher back stress against twin growth [26]. To explain the formation of the wide or multiple parallel twins in Figures 1 and 2, we also considered in simulation two parallel twins (Figure 4). The TRSS (dark blue) fields resulting from parallel twins show intense back stresses in the central region of the twins due to the mutual interaction of their stress fields. However, the twin boundary back stress has substantially reduced locally at the twin- β layer junction. The back stress is far lower than the interacting with a grain boundary [26] and remarkably, even lower than that of single twin- β layer situation (Figure S2). These results indicate that parallel twins would stimulate twin expansion where the twin meets the β layer, even more so than an isolated twin. This unusual promotion of twinning is a consequence of the enhanced localized plasticity in the vicinity of twin tip in both α and β layers (Figure 4(b,c)), which relaxes the twin boundary back stress near the twin- β junction. The prediction is consistent with the frequent observation of multiple parallel twins observed in Figure 2(f). As a result, less additional applied stress is needed for twins to further thicken when a series of parallel twins impinge on β layer. With many twins in one α layer, the extent of the forward stress generated in the next α layer has broadened, an effect that is expected to increase the likelihood of twin propagation across the laminated colony. Local twin thickening can also accelerate coalescence of these twins in the same α layer.

4. Conclusions

We report deformation twinning in a hierarchical 3D nanolayered Zr-2.5Nb. The β nanolayers played a critical role in the twinning process, enabling the twins, even an infrequent twin type, to grow to a significant extent within the colony. Twins impinging on the β layer can

trigger new twins in the next α layer, without the need to transmit dislocations through the β layer or locally twin the β layer. Thus, the twin ‘hops’ to the next α layer. After it hops, the intervening β layer then undergoes minor plasticity and helps to further drive twin thickening because it reduces the back stress compared to that provided by pure α -Zr matrix. These findings elucidate the potential of ductile nanolayering for stimulating profuse twinning, by twin hopping.

Acknowledgements

This work was supported by the National Natural Science Foundation of China (Grant Nos. 51922082, 51971170 and 51942104), the National Key Research and Development Program of China (2017YFB0702301), the 111 Project of China (Grant Number BP2018008) and the Innovation Project of Shaanxi Province (grant number 2017KTPT-12).

Disclosure statement

No potential conflict of interest was reported by the authors.

Funding

This work was supported by the National Natural Science Foundation of China [grant numbers 51922082, 51971170 and 51942104], the National Key Research and Development Program of China [2017YFB0702301], the 111 Project of China [grant number BP2018008] and the Innovation Project of Shaanxi Province [grant number 2017KTPT-12].

References

- [1] Callisti M, Polcar T. Combined size and texture-dependent deformation and strengthening mechanisms in Zr/Nb nano-multilayers. *Acta Mater.* 2017;124:247–260.
- [2] Callisti M, Karlik M, Polcar T. Competing mechanisms on the strength of ion-irradiated Zr/Nb nanoscale multilayers: interface strength versus radiation hardening. *Scr Mater.* 2018;152:31–35.

- [3] Wu SH, Cheng PM, Wu K, et al. Effect of He-irradiation fluence on the size-dependent hardening and deformation of nanostructured Mo/Zr multilayers. *Int J Plast.* **2018**;111:36–52.
- [4] Liang XQ, Wang YQ, Zhao JT, et al. Size-dependent microstructure evolution and hardness of He irradiated Nb/Zr multilayers under different ion doses. *Mater Sci Eng A.* **2019**;764:138259.
- [5] Zhang JW, Beyerlein IJ, Han WZ. Hierarchical 3D nanolayered duplex-phase Zr with high strength, strain hardening, and ductility. *Phys Rev Lett.* **2019**;122:255501.
- [6] Zhang M, Luan BF, Song ZL, et al. $\{11\bar{2}1\}$ - $\{10\bar{1}2\}$ double twinning in a Zircaloy-4 alloy during rolling at ambient temperature. *Scr Mater.* **2016**;122:77–81.
- [7] Beyerlein IJ, Zhang XH, Misra A. Growth twins and deformation twins in metals. *Annu Rev Mater Res.* **2014**;44:329–363.
- [8] Knezevic M, Zecevic M, Beyerlein IJ, et al. Strain rate and temperature effects on the selection of primary and secondary slip and twinning systems in HCP Zr. *Acta Mater.* **2015**;88:55–73.
- [9] Chai LJ, Luan BF, Xiao DP, et al. Microstructural and textural evolution of commercially pure Zr sheet rolled at room and liquid nitrogen temperatures. *Mater Des.* **2015**;85:296–308.
- [10] Fuloria D, Kumar N, Goel S, et al. Tensile properties and microstructural evolution of Zircaloy-4 processed through rolling at different temperatures. *Mater Des.* **2016**;103:40–51.
- [11] Capolungo L, Marshall PE, McCabe RJ, et al. Nucleation and growth of twins in Zr: a statistical study. *Acta Mater.* **2009**;57:6047–6056.
- [12] Khosravani A, Fullwood DT, Adams BL, et al. Nucleation and propagation of $\{10\bar{1}2\}$ twins in AZ31 magnesium alloy. *Acta Mater.* **2015**;100:202–214.
- [13] Kapoor R, Sarkar A, Singh J, et al. Effect of strain rate on twinning in a Zr alloy. *Scr Mater.* **2014**;74:72–75.
- [14] Song SG, Gray GT. Influence of temperature and strain rate on slip and twinning behavior of Zr. *Metall Mater Trans A.* **1995**;26A:2665–2675.
- [15] Han WZ, Carpenter JS, Wang J, et al. Atomic-level study of twin nucleation from face-centered-cubic/body-centered-cubic interfaces in nanolamellar composites. *Appl Phys Lett.* **2012**;100:011911.
- [16] Zheng XD, Zheng SJ, Wang J, et al. Twinning and sequential kinking in lamellar Ti-6Al-4V alloy. *Acta Mater.* **2019**;181:479–490.
- [17] Wang J, Beyerlein IJ, Mara NA, et al. Interface-facilitated deformation twinning in copper within submicron Ag-Cu multilayered composites. *Scr Mater.* **2011**;64:1083–1086.
- [18] Robson JD, Stanford N, Barnett MR. Effect of precipitate shape and habit on mechanical asymmetry in magnesium alloys. *Metall Mater Trans A.* **2013**;44A:2984–2995.
- [19] Kada SR, Lynch PA, Kimpton JA, et al. *In-situ* X-ray diffraction studies of slip and twinning in the presence of precipitates in AZ91 alloy. *Acta Mater.* **2016**;119:145–156.
- [20] Liu BY, Yang N, Wang J, et al. Insight from *in situ* microscopy into which precipitate morphology can enable high strength in magnesium alloys. *J Mater Sci Technol.* **2018**;34:1061–1066.
- [21] Wu XL, Youssef KM, Koch CC, et al. Deformation twinning in a nanocrystalline hcp Mg alloy. *Scr Mater.* **2011**;64:213–216.
- [22] Zhu YT, Liao XZ, Wu XL. Deformation twinning in nanocrystalline materials. *Prog Mater Sci.* **2012**;57:1–62.
- [23] Liu Y, Tang PZ, Gong MY, et al. Three-dimensional character of the deformation twin in magnesium. *Nat Commun.* **2019**;10:3308.
- [24] McCabe RJ, Cerreta EK, Misra A, et al. Effects of texture, temperature and strain on the deformation modes of zirconium. *Philos Mag.* **2006**;86:3595–3611.
- [25] Yu Q, Shan ZW, Li J, et al. Strong crystal size effect on deformation twinning. *Nature.* **2010**;463:335–338.
- [26] Kumar MA, Beyerlein IJ, Tome CN. Effect of local stress fields on twin characteristics in HCP metals. *Acta Mater.* **2016**;116:143–154.
- [27] Kumar MA, Gong M, Beyerlein IJ, et al. Role of local stresses on co-zone twin-twin junction formation in HCP magnesium. *Acta Mater.* **2019**;168:353–361.
- [28] Christian JW, Mahajan S. Deformation twinning. *Prog Mater Sci.* **1995**;39:1–157.
- [29] Wang L, Yang Y, Eisenlohr P, et al. Twin nucleation by slip transfer across grain boundaries in commercial purity titanium. *Metall Mater Trans A.* **2010**;41A:421–430.